PCCP

Accepted Manuscript

ROYAL SOCIETY OF CHEMISTRY

www.rsc.org/pccp

Journal Name

ARTICLE TYPE

Cite this: DOI: 10.1039/xxxxxxxxxx

Identifying and avoiding singularity-induced local traps over control landscapes of spin chain systems

Qiuyang Sun[a], István Pelczer[a], Gregory Riviello[a], Re-Bing Wu[b] and Herschel Rabitz*[a]

Received Date
Accepted Date

DOI: 10.1039/xxxxxxxxxx

www.rsc.org/journalname

The wide success of quantum optimal control in experiments and simulations is attributed to the properties of the control landscape, defined by the objective value as a functional of the controls. Prior analysis has shown that on satisfaction of some underlying assumptions, the landscapes are free of suboptimal traps that could halt the search for a global optimum with gradient-based algorithms. However, violation of one particular assumption can give rise to a so-called singular control, possibly bringing about local traps on the corresponding landscapes in some particular situations. This paper theoretically and experimentally demonstrates the existence of singular traps on the landscape in linear spin-1/2 chains with Ising couplings between nearest neighbors and with certain field components set to zero. The results in a two-spin example show how a trap influences the search trajectories passing by it, and how to avoid encountering such traps in practice by choosing sufficiently strong initial control fields. The findings are also discussed in the context of the generally observed success of quantum control.

1 Introduction

Quantum dynamics phenomena at the atomic and molecular scales can be controlled via the application of tailored electromagnetic fields.[1] The control objective, e.g., the expectation value of an observable, can be optimized by shaping the control fields. A *control landscape* is defined by the objective value J as a functional of the controls, whose topology dictates the ease of finding the globally optimal solutions, especially when using gradient-based search algorithms. What lies at the core of control landscape analysis is the local topology around its suboptimal critical (or stationary) points, which is assessed primarily by a second derivative test, i.e., the definiteness of the *Hessian* matrix evaluated at a critical point. In this paper, a suboptimal critical point with a nonzero and negative semidefinite Hessian is referred to as a *trap* for maximization of J, although it is not necessarily a local maximum when the Hessian has a nonempty null space (or kernel). More rigorously, such critical points are traps of at least second order, and behave similarly to local maxima for optimization algorithms utilizing first- and second-order derivatives only.[2–4] Based on the assumptions that (i) the closed quantum system is controllable,[5–7] (ii) the control to final state map is surjective everywhere over the landscape,[2,8,9] and (iii) the control fields are unconstrained, theoretical analyses reveal that the landscape is free of any traps,[10–12] i.e., a gradient search will converge to a globally optimal solution from an arbitrary initial choice in the space of control fields. The trap-free landscape conclusion is a fortunate fiducial outcome of fully satisfying the three assumptions stated above, which provides a basis to understand the observed generally successful outcomes of quantum optimal control in both experiments[1] and simulations.[13] In particular circumstances the assumptions may be only partially satisfied, which can lead to additional landscape features appearing, including traps. In practice, satisfaction of assumption (iii) to an adequate degree is of concern and has been the focus of recent studies.[14–16] Notwithstanding the overall growing numbers of positive control experiments, each of the assumptions deserve additional analysis to assess their ease of practical satisfaction.

This paper focuses on so-called *singular* controls, which locally violate the assumption (ii) above and may produce suboptimal traps on the landscape. This prospect was considered earlier,[17] and a few special examples of local traps based on theoretical model systems have been reported,[2,18] which can be ascribed to singularity. A general basis to assess the role of singular controls has been established in Ref.[8]. Carefully performed numerical simulations suggest that the singular controls are very rare, and most of them actually do not form traps for gradient searches.[8,9] The singular traps known so far are associated with zero (or constant) fields,[2,18] and have very small attractive volumes, i.e., a search is likely to be halted in practice only if the initial control is chosen sufficiently close to the exact singular trap.[9,19] This circumstance also applies to the findings in this paper, but the possible pres-

[a] Department of Chemistry, Princeton University, Princeton, New Jersey 08544, USA. E-mail: hrabitz@princeton.edu
[b] Department of Automation, Tsinghua University and Center for Quantum Information Science and Technology, TNList, Beijing, 100084, China

ence of such traps and the means for their avoidance is a matter of considerable interest.

The control of dynamics in coupled spin-1/2 chains is of both theoretical and practical interest,[20] because of its proposed utility in various applications including for efficient transfer of information in quantum computing devices,[21] and in signal enhancement by polarization transfer in nuclear magnetic resonance (NMR) spectroscopy.[22] Analysis of the underlying control landscape structures could be valuable in these situations. Recently we developed experimental methodology for studying the control landscape of spin systems with NMR.[23,24] This paper focuses on the singular traps in control landscapes arising in linear spin chains and the associated influence of non-local spin couplings. Unlike many previous studies[2,8–11,18] in which only a *single* control field was considered, the complete controllability of a multispin system generally calls for the introduction of *multiple* control fields when each spin is spectrally distinct from the others. In this situation, singularity may exist at special controls where some of the field components have zero value, which in turn may convert a regular landscape saddle point with an indefinite Hessian to a second-order local trap.

The remainder of the paper is organized as follows. Section 2 provides the theoretical background for control landscapes and singular controls. Section 3 analyzes a particular landscape problem defined in linear spin chain systems and specifies the conditions for a singular control to become a local trap. Illustrative examples for a two-spin system are given in Section 4 with experimental and simulational results, confirming the existence of the singular traps and showing how to avoid them in practice by appropriate choices of initial controls. While the analysis in the paper mainly focuses on spin chains with nearest neighbor couplings, treatment of a three-spin system with next nearest neighbor coupling demonstrates a reduction in singular behavior. Finally, Section 5 gives general conclusions and also discusses the overall special circumstances of zero (or constant) field singular controls, in the backdrop of the general success of quantum control experiments and the trap-free findings in large numbers of carefully performed simulations.[13,25]

2 Control landscape and singular controls

Consider a closed N-level quantum system under control, whose dynamics is described by the time-dependent Schrödinger equation (in units where $\hbar = 1$),

$$i\frac{d}{dt}U(t) = \left[H_0 + \sum_{m=1}^{M} u_m(t)H_m\right]U(t), \quad U(0) = \mathbb{I}_N, \qquad (1)$$

where H_0 is the internal Hamiltonian, $H_1, \cdots, H_M$ are the linearly independent interaction Hamiltonian terms, and $u_1(t), \cdots, u_M(t)$ are their corresponding control fields, defined on the time interval $t \in [0, T]$. In the following we will encapsulate all of the M control fields into an entire dynamic control $u(\cdot)$ when necessary, and each u_m will be called a *component* of it. The circumstance in eqn (1) arises in the present work with a set of weakly coupled spins where each spin is spectrally distinguishable from the others and thus may be individually addressed. A necessary and sufficient condition for complete controllability of the system is that the Lie algebra generated by iH_0 and iH_m, $m = 1, \cdots, M$, is u(N) (or su(N) for a traceless Hamiltonian).[5,6] The density matrix ρ, denoting the system state, evolves with time as $\rho(t) = U(t)\rho(0)U^\dagger(t)$, or equivalently obeys the Liouville-von Neumann equation

$$\frac{d}{dt}\rho(t) = -i\left[H_0 + \sum_{m=1}^{M} u_m(t)H_m, \rho(t)\right]. \qquad (2)$$

For a system with a given initial state $\rho(0)$, a widely studied target of quantum control is to optimize the expectation value of a Hermitian observable operator O at the final time T.[11,12,26] The objective J specifies the landscape as a functional of the control $u(\cdot)$ through $U(T)$, expressed by

$$J = \mathrm{Tr}[\rho(T)O] = \mathrm{Tr}[U(T)\rho(0)U^\dagger(T)O]. \qquad (3)$$

In order to simplify the analysis of the *dynamic* landscape (i.e., J as a functional of the control fields), the *kinematic* picture of the landscape is introduced, which is only concerned with the system state $\rho(T)$ at the final time T, but not the dynamics leading to the final state. Thus, in the kinematic picture the landscape J is simply treated as a function of $\rho(T)$ defined on the space of matrices unitarily equivalent to $\rho(0)$, or a function of $U(T)$ defined on the unitary group U(N).[8,12,26] Landscape analysis primarily aims at identifying the *critical points* where the first derivative of J is zero, which can slow down or even halt the gradient-based optimization searches. The first derivative of J in the dynamic and kinematic landscapes are related through the chain rule

$$\frac{\delta J}{\delta u(\cdot)} = \left\langle \nabla J[\rho(T)], \frac{\delta \rho(T)}{\delta u(\cdot)} \right\rangle_{\rho(T)}, \qquad (4)$$

where $\langle \cdot, \cdot \rangle$ represents the Riemannian metric, $\nabla J[\rho(T)]$ is the kinematic gradient of J, and $\frac{\delta \rho(T)}{\delta u(\cdot)}$, which can be interpreted as a *Jacobian* matrix, is the state variation at T resulted from a variation $\delta u(\cdot)$ in the control space.[8] When $\frac{\delta \rho(T)}{\delta u(\cdot)}$ is full rank (i.e., the set $\frac{\delta \rho_{jk}(T)}{\delta u(\cdot)}$, $\forall j$ and k, contains the maximal allowed number of linearly independent functions), we have $\frac{\delta J}{\delta u(\cdot)} = 0$ if and only if $\nabla J[\rho(T)] = 0$. A criterion for a particular $\rho(T)$ to be such a kinematic critical point (KCP), is that[11]

$$[\rho(T), O] = 0. \qquad (5)$$

Further analysis reveals that the topology of the kinematic landscape is determined solely by the initial state $\rho(0)$ and target observable O, and KCPs occur at specific discrete values of J, which can be computed from the eigenvalues of $\rho(0)$ and O.[11] The local landscape topology about a critical point is assessed by the definiteness of its Hessian. By analyzing the kinematic Hessian form, i.e., the second derivative of J with respect to $\rho(T)$, it can be shown that all the suboptimal KCPs located between the global maximum and minimum of the landscape, if any, must have both positive and negative Hessian eigenvalues, and thus be *saddle points*.[12] Therefore, the kinematic landscape does not contain any local traps for optimization searches.

The viability of lifting the landscape analysis results in the kine-

matic picture to the dynamic picture can be guaranteed if the Jacobian $\frac{\delta\rho(T)}{\delta u(\cdot)}$ is full rank,[26] and such controls and critical points are called *regular*. In contrast, a dynamic control $u(\cdot)$ is referred to as *singular* if the Jacobian is rank deficient,[8] in which case the final state $\rho(T)$ cannot be freely manipulated differentially by perturbing the control fields. The rank deficiency of $\frac{\delta\rho(T)}{\delta u(\cdot)}$ is called the *corank* of a singular control, characterizing the degree of its singularity.[8] Singularity can lead to changes of local landscape topology from at least two perspectives. First, it can induce nonkinematic critical points (NKCPs) on the dynamic landscape, which do not satisfy the condition in eqn (5) and therefore have no counterparts in the kinematic picture. Although these singular NKCPs are dominantly saddles,[8,9] special examples are known in which the singular NKCPs have negative definite or semidefinite Hessians.[18] Second, singularity can qualitatively alter the Hessian feature at a KCP, where the second derivative of J in the two pictures is related by[8,26]

$$\frac{\delta^2 J}{\delta u^2(\cdot)} = \left\langle \frac{\delta\rho(T)}{\delta u(\cdot)}, \mathbb{Q}_{\rho(T)} \frac{\delta\rho(T)}{\delta u(\cdot)} \right\rangle_{\rho(T)}, \tag{6}$$

where $\mathbb{Q}_{\rho(T)}$ is the kinematic Hessian of J at $\rho(T)$. The nonzero eigenvalues of $\mathbb{Q}_{\rho(T)}$ are mapped one-to-one to the dynamic picture if $\frac{\delta\rho(T)}{\delta u(\cdot)}$ is full rank, but a dynamic critical point may lose some nonzero Hessian eigenvalues of its kinematic counterpart when it is singular. In some extreme cases, a kinematic saddle point can even be converted to a dynamic second-order maximum if all the positive Hessian eigenvalues vanish due to singularity.[2,19] The situation analyzed in the following section will also fall into this category. To our knowledge, some of the singularity-induced traps discovered to date are true local maxima with strictly negative definite Hessians,[18] while the others recover the topology of saddles when higher-order derivatives are further considered,[2,18,19] including the case studied in this paper. The local landscape topology at singular controls is related to the nature of the controlled quantum system in a complex and subtle manner.

3 Singular traps in linear spin chain systems

3.1 Control system model and landscape gradient search.

This paper mainly addresses the model system of a linear chain consisting of n spins-1/2 with Ising-type coupling, also known as weak coupling in NMR,[20] only between nearest neighbors; the consequences of additional spin coupling complexity are discussed in Sections 3.3 and 5. We assume that the Larmor frequencies of the spins are well separated, so that each spin can be individually addressed by its on-resonance control field. A multiple rotating frame[27] simultaneously operating at the resonance frequencies of each spin is introduced to express the total Hamiltonian of the controlled system as (in units where $\hbar = 1$)

$$H(t) = \sum_{j=1}^{n-1} J^{j,j+1} I_z^j I_z^{j+1} + \sum_{j=1}^{n} \left[u_x^j(t) \cdot I_x^j + u_y^j(t) \cdot I_y^j \right], \tag{7}$$

where $J^{j,j+1}$ is the coupling strength between the spins j and $j+1$ in units of frequency. The multispin operator I_a^j $(a = x,y,z)$ denotes the tensor product of the single-spin operator σ_a for the jth spin with identity operators for all the others:[28,29]

$$I_a^j = \underbrace{\mathbb{I}_2 \otimes \cdots \otimes \mathbb{I}_2}_{j-1} \otimes (\sigma_a/2) \otimes \underbrace{\mathbb{I}_2 \otimes \cdots \otimes \mathbb{I}_2}_{n-j}, \tag{8}$$

where σ_a $(a = x,y,z)$ is a Pauli matrix and $\mathbb{I}_2$ is the 2×2 identity matrix. The products of the operators I_a^j with different spin labels j, such as $I_x^1 I_y^2$, form an orthogonal basis for traceless 2^n-dimensional Hermitian matrices.[28] The control portion of the Hamiltonian includes $2n$ linearly independent terms associated with the operators I_x^j and I_y^j $(j = 1,\cdots,n)$, each addressed by a corresponding field $u_x^j(t)$ or $u_y^j(t)$ in units of frequency. The quantum system is completely controllable with the Hamiltonian form of eqn (7).[5,6]

For a specific control landscape problem in this system, we consider an initial density matrix with its traceless portion having the form $\rho(0) = \sum_{j=1}^{n} c_j I_z^j$ $(c_j > 0)$, which well approximates the thermal equilibrium state of n spectrally distinguishable spins with gyromagnetic ratios proportional to the c_j's, in conventional NMR experiments when the system is placed in a large static magnetic field along the z direction.[30] The observable is chosen as $O = I_x^k$, $k \in \{1,\cdots,n\}$, which targets the in-phase coherence in the x direction of the kth spin.[28] We will refer to the kth spin as the *target* spin, and all the others in the chain as *spectator* spins when necessary. A complete list of KCPs over this landscape will not be given here; we only point out that there exist critical points at $J = \pm 2^{n-2} c_j$, $\forall j = 1,\cdots,n$ (2^{n-2} is a coefficient arising from the number of spins n in the system), most of which [a] have to be suboptimal saddle points in the kinematic picture.[11,12] The landscape settings described here can be realized by heteronuclear NMR experiments in a straightforward manner; a two-spin example will be presented in Section 4.

The landscape analysis of our problem will start with gradient-based optimization of each single field component at some special dynamic controls. Invoking eqns (1) and (2), the gradient of the objective $J = \mathrm{Tr}[\rho(T)O]$ with respect to a single field $u_m(t)$ is given by[11,31]

$$\frac{\delta J}{\delta u_m(t)} = -i\mathrm{Tr}\left\{ [\rho(t), U(t)U^\dagger(T)OU(T)U^\dagger(t)] H_m \right\}. \tag{9}$$

For the observable $O = I_x^k$ and for a dynamic control with all the field components set to zero except $u_y^k(t)$, the gradient with respect to each of the $(2n-1)$ zero fields will still be zero, as demonstrated below. In this special case, the total Hamiltonian reduces to

$$H(t) = \sum_{j=1}^{n-1} J^{j,j+1} I_z^j I_z^{j+1} + u_y^k(t) \cdot I_y^k. \tag{10}$$

Thus, the terms $\rho(t)$ and $U(t)U^\dagger(T)OU(T)U^\dagger(t)$ in the gradient

[a] Only the critical points of the greatest c_j might be the top and bottom, but in some cases the actual top and bottom can still exceed them and do not belong to the category $J = \pm 2^{n-2} c_j$, as Section 3.3 shows in the three-spin case.

formula of eqn (9) can only evolve in some Hermitian subspaces. The time evolution of $\rho(t)$ from $\rho(0)=\sum_{j=1}^{n} c_j I_z^j$, obeying eqn (2) with $H(t)$ given in eqn (10), is constrained within the subspace spanned by the following product operators,

$$\rho(t) \in \text{span}\{I_z^j (j=1,\cdots,n), I_x^k, I_y^k I_z^{k\pm1}, I_z^{k-1} I_x^k I_z^{k+1}, I_z^{k-1} I_z^k I_z^{k+1}\},$$

which is determined by calculating the commutator of $\rho(t)$ with $H(t)$, starting from $\rho(0)$, until no more linearly independent terms can be added in. Since $U(t)U^\dagger(T)OU(T)U^\dagger(t)$ is the unitary evolution of $O=I_x^k$ governed by the Hamiltonian of eqn (10), we can also derive the corresponding subspace as

$$U(t)U^\dagger(T)OU(T)U^\dagger(t) \in \text{span}\{I_x^k, I_z^k, I_y^k I_z^{k\pm1}, I_z^{k-1} I_x^k I_z^{k+1}, I_z^{k-1} I_z^k I_z^{k+1}\}.$$

Among the $2n$ distinct H_m terms of eqn (9), $H_m \in \{I_x^j, I_y^j\}_{j=1}^n$, only I_y^k is present in the domain of $[\rho(t), U(t)U^\dagger(T)OU(T)U^\dagger(t)]$, so the landscape gradients with respect to control field components set *a priori* to zero [other than $u_y^k(t)$] all vanish. Thus, we have

Remark 1. When starting from an initial control with $u_y^k(t)$ being the only nonzero field, the other $(2n-1)$ zero components will permanently stay at zero throughout an optimization process utilizing a simple gradient ascent algorithm [see eqn (19) in Section 4]. Likewise, if $u_x^k(t)$ and $u_y^k(t)$ are the only nonzero components in the initial control, the remaining $(2n-2)$ fields will stay at zero during a gradient ascent, which can be demonstrated in the same manner.

As such, although we have sufficient control resources, we will never get the chance to utilize all of them for some special initial control guesses. The consequence is that the special search trajectories may converge to suboptimal critical points, instead of the global optimum. When the control fields addressing the $(n-1)$ spectator spins are all zero, the terms I_z^j $(j \neq k)$ in the initial state $\rho(0)$ will stay invariant throughout the control duration since they commute with the total Hamiltonian, and have no contribution to the observable $O=I_x^k$. In that case, the objective function $J=\text{Tr}[\rho(T)O]$ reduces to

$$J[U(T)] = c_k \text{Tr}[U(T) I_z^k U^\dagger(T) I_x^k]. \tag{11}$$

The range of this function is $2^{n-2}[-c_k, c_k]$. The values $J=\pm 2^{n-2}c_k$ correspond to KCPs of the original landscape, but not the global maximum or minimum in most cases. Therefore,

Remark 2. Gradient ascent from an initial control with field components on all spectator spins being zero will converge to a KCP at $J=2^{n-2}c_k$, which is usually suboptimal.

In Section 3.2 we will determine whether such an end point is a saddle or a second-order trap in the dynamic picture by analyzing its Hessian matrix.

3.2 Hessian analysis at the singular critical point.

For the landscape involving M $(=2n$ in our spin chain system) independent control fields, the entire Hessian $\mathbb{H}(t,t')$ is specified as a real symmetric matrix composed of $M\times M$ submatrices $\mathbb{H}_{mm'}(t,t')$, with each of infinite dimension over the time domain $[0,T]$. An off-diagonal submatrix $\mathbb{H}_{mm'}$ with $m\neq m'$ is generally nonsymmetric by itself, but is the transpose of its opposite submatrix $\mathbb{H}_{m'm}$. In each submatrix, the triangular portion of the domain $0\le t'<t\le T$ is given by[11,32]

$$\mathbb{H}_{mm'}(t,t') := \frac{\delta^2 J}{\delta u_m(t)\delta u_{m'}(t')} = -\text{Tr}\{[[O(T), H_m(t)], H_{m'}(t')]\rho(0)\} \tag{12}$$

for $m,m'=1,\cdots,M$, and the opposite triangular portion can be determined by symmetry, $\mathbb{H}_{mm'}(t',t)=\mathbb{H}_{m'm}(t,t')$. The operators $O(T)$ and $H_m(t)$ are defined with the system dynamics in the Heisenberg picture, i.e., $O(T):=U^\dagger(T)OU(T)$ and $H_m(t):=U^\dagger(t)H_mU(t)$. For our specific problem we conclude:

Remark 3. On the landscape $J=\text{Tr}[O(T)\rho(0)]$ with the Hamiltonian given in eqn (7) and $\rho(0)=\sum_{j=1}^n c_j I_z^j$, $O=I_x^k$, a dynamic control must have a negative semidefinite Hessian if it satisfies two conditions: (i) all the field components except $u_y^k(t)$ are zero, and (ii) $O(T)=I_z^k$. Invoking eqns (3) and (5), condition (ii) implies that such a control corresponds to a KCP lying at $J=2^{n-2}c_k$.

Proof. The analysis below is carried out via a semi-explicit expression of each Hessian submatrix at a control satisfying the two conditions. With the Hamiltonian of eqn (10) involving a nonzero control $u_y^k(t)$ only, the time evolution of the operator $I_y^k(t)=U^\dagger(t)I_y^kU(t)$, for example, can be expressed as

$$I_y^k(t) = a_1\cdot I_y^k + a_2\cdot 2I_z^{k-1}I_x^k + a_3\cdot 2I_x^k I_z^{k+1} + a_4\cdot 4I_z^{k-1}I_y^k I_z^{k+1} + a_5\cdot 2I_z^{k-1}I_z^k + a_6\cdot 2I_z^k I_z^{k+1}, \tag{13}$$

where $a_1,\cdots,a_6$ are all real scalar functions of t. With the condition $O(T)=I_z^k$, we calculate the diagonal Hessian submatrix $\mathbb{H}_{mm'}$ with $H_m=H_{m'}=I_y^k$ by eqn (12):

$$[O(T), I_y^k(t)] = i[-a_1(t)\cdot I_x^k + a_2(t)\cdot 2I_z^{k-1}I_y^k + a_3(t)\cdot 2I_y^k I_z^{k+1} - a_4(t)\cdot 4I_z^{k-1}I_x^k I_z^{k+1}], \tag{14}$$

$$\frac{\delta^2 J}{\delta u_y^k(t)\delta u_y^k(t')} = -2^{n-2}c_k[a_1(t)a_1(t') + a_2(t)a_2(t') + a_3(t)a_3(t') + a_4(t)a_4(t')], \quad t,t'\in[0,T]. \tag{15}$$

Hence, the subspace of the field component $u_y^k(t)$ gives four negative Hessian eigenvalues, whose corresponding eigenvectors are specified by linear combinations of the functions $a_1(t)$, $a_2(t)$, $a_3(t)$ and $a_4(t)$. If we perturb the field $u_y^k(t)$ and keep the other $(2n-1)$ components invariant at zero value at the critical point, the J value will drop quadratically if and only if the variation $\delta u_y^k(t)$ has a nonzero projection on the linear space spanned by the four functions above. Similarly, the field $u_x^k(t)$ also has four negative

Hessian eigenvalues associated with it.

Regarding the two nearest neighbors of the target spin k, the time evolution of $I_{x/y}^{k\pm1}(t)$ under eqn (10) can be formulated as well, e.g.,

$$\begin{aligned} I_x^{k-1}(t) &= b_1\cdot I_x^{k-1}+b_2\cdot 2I_z^{k-2}I_y^{k-1}+b_3\cdot 2I_y^{k-1}I_z^{k}+b_4\cdot 4I_z^{k-2}I_x^{k-1}I_z^{k}+b_5\cdot 2I_y^{k-1}I_x^{k}+ \\ &\quad +b_6\cdot 4I_z^{k-2}I_x^{k-1}I_x^{k}+b_7\cdot 4I_y^{k-1}I_y^{k}I_z^{k+1}+b_8\cdot 8I_z^{k-2}I_x^{k-1}I_y^{k}I_z^{k+1}, \end{aligned} \tag{16}$$

where $b_1,\cdots,b_8$ are functions of t. Likewise,

$$\frac{\delta^2 J}{\delta u_x^{k-1}(t)\delta u_x^{k-1}(t')} = -2^{n-2}c_k[b_5(t)b_5(t')+b_6(t)b_6(t')+b_7(t)b_7(t')+b_8(t)b_8(t')], \quad t,t'\in[0,T]. \tag{17}$$

We find that the control subspace of the field $u_x^{k-1}(t)$ also contains four Hessian eigenvectors with negative eigenvalues, given by linear combinations of $b_5(t)$, $b_6(t)$, $b_7(t)$ and $b_8(t)$. Similar situations occur for the field components $u_y^{k-1}(t)$, $u_x^{k+1}(t)$ and $u_y^{k+1}(t)$, while the fields addressing spins other than k and $k\pm1$ have zero contribution to the entire Hessian. It is also confirmed that the off-diagonal Hessian submatrices are all zero under conditions (i) and (ii), i.e., $\delta^2 J/\delta u_m(t)\delta u_{m'}(t')\equiv 0$ if u_m and $u_{m'}$ are two different components. Therefore, the entire Hessian is semidefinite and has totally *at most* 24 negative eigenvalues, whose eigenvectors are associated with the control fields addressing the six operators $I_{x/y}^k$ and $I_{x/y}^{k\pm1}$. Q.E.D.

Unless $J=2^{n-2}c_k$ is the global maximum of the landscape, the results here demonstrate the existence of a suboptimal trap of at least second order. If we keep $O(T)=I_z^k$ and alter the circumstances in either of the two ways, (i) making the component $u_x^k(t)$ also nonzero, or (ii) adding a new coupling term $J^{k-1,k+1}I_z^{k-1}I_z^{k+1}$ into the Hamiltonian, which couples the two nearest neighbors of the target spin, the simple Hessian structure as in eqns (15) and (17) will become more complex, and no longer be necessarily negative semidefinite. In those situations the existence of second-order traps cannot be guaranteed.

If the chain is not sufficiently long at least on one side of the target spin k, when any of the four spins labeled $(k\pm1)$ or $(k\pm2)$ do not exist, the trap control may have less than 24 negative Hessian eigenvalues. For instance, if the chain contains a spin $(k+1)$ but not $(k-1)$, the terms of $I_y^k(t)$ in eqn (13) with coefficients a_2, a_4 and a_5 will disappear, and the subspace of $u_y^k(t)$ will give only two (instead of four) negative eigenvalues whose eigenvectors are linear combinations of $a_1(t)$ and $a_3(t)$. The numbers of negative Hessian eigenvalues, $\mathbb{D}_-$, for different spin chain structures are counted with the method above and summarized in Table 1. Since only the five spins from $(k-2)$ to $(k+2)$ participate in the Hessian calculation, the presence of more spins in the chain will have no influence on the Hessian structure of our control problem targeting spin k.

The emergence of the second-order trap on the landscape, as expected, is closely related to singularity, or the rank deficiency of $\frac{\delta\rho(T)}{\delta u(\cdot)}$, which can be calculated by[8]

$$\frac{\delta\rho(T)}{\delta u_m(t)} = -iU(T)[H_m(t),\rho(0)]U^\dagger(T), \quad H_m\in\{I_x^j,I_y^j\}_{j=1}^n. \tag{18}$$

Numerical simulations in two- and three-spin systems show that any dynamic control with only one of the $2n$ field components turned on should be singular (see Sections 3.3 and 4 for details). Although singular controls of this type can bring about new topological features, i.e., suboptimal second-order traps, to the dynamic landscape when overlapping with the kinematic saddle points, their significance in practice calls for special consideration, as starting with zero field components is not physically reasonable in a coupled spin system. The latter issue is examined in Section 4 and in ref.[9] for other like situations, as the domain of "attraction" around a trap is of primary importance.

Table 1 Dependence of the number of negative Hessian eigenvalues at the local second-order trap, $\mathbb{D}_-$, on the number of spins in the chain on both sides of the spin k targetd by the observable $O=I_x^k$. The target spin is represented by • and the other spectator spins by ○. Furthermore, $\cdots$ means that adding any more spins on that side does not change the Hessian index $\mathbb{D}_-$.

Spin chain structure	$\mathbb{D}_-$
•	2
•-○	6
•-○-○$\cdots$	8
○-•-○	16
○-•-○-○$\cdots$	20
$\cdots$○-○-•-○-○$\cdots$	24

3.3 The influence of more complex coupling in a three-spin case.

The simple nearest neighbor coupling structure of the linear chain model considered here is crucial for the existence of the singular traps, as shown by the following example in the three-spin case. Consider a control landscape with $\rho(0)=I_z^1+0.8I_z^2+0.6I_z^3$ and $O=I_x^2$, defined in a linear chain model where spin 2 is coupled with its two (uncoupled) neighbors, spins 1 and 3. The condition (ii) in *Remark 3*, $O(T)=I_z^2$, identifies a KCP lying at $J=1.6$ com-

pared to the global maximum $J = 2.4$,[11] whose kinematic Hessian form should have 6 positive and 26 negative eigenvalues.[12] On further satisfaction of condition (i), the corresponding singular dynamic critical point will have a semidefinite Hessian with 16 negative eigenvalues, and thus form a second-order trap. However, with the appearance of an additional next nearest neighbor coupling (i.e., triangular coupling) term $J^{1,3}I_z^1 I_z^3$ in the Hamiltonian, a control satisfying the two conditions will still be critical but have an indefinite Hessian with 4 positive and 20 negative eigenvalues, being a saddle on the dynamic landscape instead of a second-order maximum. We see that the more complex coupling gives a lower degree of singularity, or Jacobian corank (cf. Section 2) at the same special dynamic control, which consequently influences the local landscape topology. In this example the Hessians are numerically computed with eqn (12), with the coupling constants $J^{1,2}$, $J^{2,3}$ and $J^{1,3}$ set to be unequal. Section 5 contains further discussion on the role of coupling structure upon landscape topology.

4 Illustrations

In this section we demonstrate the existence of singular suboptimal traps in a two-spin systems as illustrations. We present experimental results and numerical simulations for a heteronuclear two-spin sample ($^{13}CHCl_3$), revealing how the choice of initial controls influences the likelihood of trapping in practice.

The gradient algorithm used for ascending the landscape and searching for the critical points is described below. In optimal control experiments and simulations of a quantum system with dynamics having the form of eqn (1), the objective function J can be optimized by updating the control field(s) iteratively along the gradient flow, until a critical point is encountered.[9,19,31] We introduce a scalar parameter $s \geq 0$ to describe the evolution of a control field $u_m(s,t)$ in the landscape ascent process, which is guided by the differential equation

$$\frac{\partial u_m(s,t)}{\partial s} = \alpha_m(s)\frac{\delta J}{\delta u_m(s,t)}, \tag{19}$$

where $\alpha_m > 0$ is the optimization rate associated with u_m. We discretize the nominally smooth field $u_m(t)$ to a piecewise constant function of L time intervals with identical length $\Delta t = T/L$, and denote the field value within the lth interval ($l = 1, \cdots, L$) by $u_m[l]$, where s is implicit. The differential equation (19) can be approximately solved by the forward Euler method with a constant step size, i.e.,

$$u_m[k+1,l] = u_m[k,l] + \alpha_m \frac{\partial J}{\partial u_m[l]}\bigg|_k. \tag{20}$$

where $k = 0, 1, \cdots$ is the iteration index. In the laboratory, the partial derivatives $\frac{\partial J}{\partial u_m[l]}$ can be measured by the central finite difference method[23] if the signal-to-noise ratio is sufficiently high, while in simulation they are approximated by the analytic gradient, given in eqn (9), at the instants $t = l\Delta t$, i.e., $\frac{\partial J}{\partial u_m[l]} \approx \Delta t \cdot \frac{\delta J}{\delta u_m(l\Delta t)}$. Depending on application, higher-order (local) integration methods may also be utilized,[19] although such techniques may be problematic to implement in the laboratory.

Here we will study the role of the singular local trap on a particular landscape in the simplest system of two coupled spins, illustrated experimentally and complemented with simulations. We consider neat ^{13}C-labeled chloroform ($^{13}CHCl_3$) as the sample,[24] and denote the two nuclei ^{1}H and ^{13}C as spin 1 and 2, respectively. The coupling strength between the two spins is $J^{1,2}/2\pi = 215$Hz, measured from the frequency difference of the two lines of the doublet ^{13}C signal in the NMR spectrum. Two radiofrequency pulses as the control resources irradiate the sample simultaneously, with each pulse on resonance with ^{1}H or ^{13}C, respectively, having a fixed length of $T = 5$ms along with time-dependent envelope amplitudes A_1, A_2 and phases ϕ_1, ϕ_2. A doubly frame rotating at resonance with the Larmor frequencies of the two spins is constructed such that the nominal controls in eqn (7) are realized by $u_x^1(t) := A_1(t)\cos\phi_1(t)$, $u_y^1(t) := A_1(t)\sin\phi_1(t)$, and similarly for u_x^2 and u_y^2.[23,24] The final time T is chosen such that $J^{1,2}T > 2\pi$ for the sake of system controllability,[29,33] and T is broken into $L = 5$ time intervals, giving a total of 20 control variables. In the rotating frame, the full Hamiltonian of the controlled system is formulated as[31]

$$H(t) = J^{1,2}I_z^1 I_z^2 + u_x^1(t)\cdot I_x^1 + u_y^1(t)\cdot I_y^1 + u_x^2(t)\cdot I_x^2 + u_y^2(t)\cdot I_y^2. \tag{21}$$

The traceless portion of the thermal equilibrium state at the experimental temperature (295 K) can be well approximated by the form $\rho_{eq} \approx c_1 I_z^1 + c_2 I_z^2$, which is taken as the initial density matrix $\rho(0)$ of the landscape problem. For the sample molecule we have $c_1 : c_2 \approx 4 : 1$, determined by the intrinsic gyromagnetic ratios of ^{1}H and ^{13}C.[27] The observable $O = I_x^2$ is characterized by the integrated area of the doublet peak ascribed to the ^{13}C nucleus (the splitting is caused by its coupling with ^{1}H) in the ^{13}C-detected NMR spectrum. With these choices of $\rho(0)$ and O, the landscape $J = \mathrm{Tr}[\rho(T)O]$ will possess KCPs at $J = \pm c_1$, $\pm c_2$, and 0, with $\pm c_1$ being the global maximum and minimum.[11]

From the landscape features at the special dynamic controls analyzed in Section 3, we can predict the general behavior of gradient optimization starting from various special initial guesses as explained below, which will be illustrated both experimentally and with simulations. (i) If we perform landscape gradient ascent from initial controls for which $u_x^1, u_y^1, u_x^2 \equiv 0$, the search trajectory will converge to a suboptimal critical point located at $J = c_2$, which is proved to be a second-order trap on the dynamic landscape. If the initial control only has $u_x^1, u_y^1 \equiv 0$, the search will also converge to $J = c_2$, but the critical point should have the topology of a saddle in this case. With such special initial controls, the zero field components in the initial control will permanently stay at zero during optimization with the gradient algorithm, and the global maximum of the landscape at $J = c_1$ cannot be approached. (ii) When the initial control is chosen to be close to the special zero field conditions in (i) leading to a trap or a saddle, the search is expected to slow down around $J = c_2$, and then speed up after escaping the neighborhood of the critical point. Under practical conditions when experimental or numerical error is present, the determination of an extremely small gradient could be inaccurate, and the search trajectory may wander randomly in a small region around the critical point. Other stochastic search methods (e.g., a genetic algorithm) may always be used,

but they generally will not reveal subtle landscape features. (iii) When the initial control is far from the special conditions, e.g., each of the four components has a significant initial magnitude, the search trajectory will likely converge to the global maximum straightforwardly without halting at any suboptimal near-critical region. The suppositions in (ii) and (iii) are based on considering that the domain of attraction for the zero field induced singular trap is small on the scale of optimal field strengths, which will be affirmed below.

The distinct behavior described above is illustrated with three search trajectories starting from different initial controls in the laboratory utilizing the gradient algorithm (see Fig. 1). We use the mean absolute value of u_m, rescaled in units of $T^{-1} = 1/(5\text{ms})$ by referring to the experimentally determined amplitude of a $\pi/2$ pulse for ^{13}C, to characterize the magnitude of each control field component, i.e., $\overline{|u_m|} = \sum_{l=1}^{L} |u_m[l]|/L$. The trajectories #1, #2 and #3 in Fig. 1 are initialized as follows: constant fields are picked as the initial control, i.e., $u_m[1] = \cdots = u_m[L] = u_{0,m}$, $m = 1, \cdots, 4$; from trajectories #1, #2 to #3, each $u_{0,m}$ increases accordingly with the ratio $0.25 : 0.58 : 1$. Although exact zero fields was not chosen, trajectory #1 started at relatively small values. Despite the J values at the initial guesses all being close to zero in Fig. 1(a), the three trajectories evolve toward different destinations under the deterministic gradient algorithm. Trajectory #1 with the lowest initial field magnitude was manually terminated when its monotonicity broke, i.e., the J value of the last iteration was slightly lower than that of its previous iteration, indicating that the system precision and noise levels were reached. Fig. 1(b) for trajectory #1 shows that in the optimization process, the magnitudes of u_x^1, u_y^1 and u_x^2 stayed at relatively low levels compared with u_y^2. Thus, the movement of trajectory #1 in the control space was stopped somewhere in the neighborhood of the predicted local trap, for which the three components other than u_y^2 should be exactly zero. In trajectory #2 as shown in Fig. 1(c), escaping the near-critical region in iterations 10-15 was accompanied by a dramatic increase of the magnitudes of u_x^1, u_y^1 and u_x^2, which can be viewed as a deviation from the trap condition. Trajectory #3, depicted in Fig. 1(d), with highest initial control magnitudes more efficiently passed through the level of J where the trap exists, and converged to the global maximum within fewer iterations than trajectory #2. The J value where trajectory #1 is terminated and #2 slows down is approximately one-fourth of the global maximal value, in agreement with the relative positions of the two KCPs at $J = c_1$ and c_2 on the landscape.

Employing numerical simulation, we also assess the likelihood of an optimization search being "trapped" under convergence criteria based on the norm of landscape gradient, with the constraints on control resources (i.e., a set number L of control variables) taken into consideration. In parallel with the experimental two-spin system, we set the J-coupling strength to $J^{1,2}/2\pi = 215$Hz and the final time to $T = 5$ms (digitized into either $L = 5$ or 10 equal time intervals). The initial state is chosen as $\rho(0) = I_z^1 + 0.25 I_z^2$, and the observable is $O = I_x^2$. The forward Euler method with a constant step size as in eqn (20) is utilized for ascending the landscape, in which the gradient with respect to the piecewise constant fields is approximated from the analytical expression in (9). The initial controls are generated by random numbers uniformly distributed around zero for each of the $4L$ control variables, and the mean absolute value $\overline{|u_m|}$ of each of the four components, u_x^1, u_y^1, u_x^2 and u_y^2, is normalized to the same value u_0 (i.e., all the L control variables of each field u_m are proportionally rescaled such that $\overline{|u_m|} = u_0$). An optimization process is terminated when the gradient norm e becomes lower than a convergence threshold, chosen over the window $10^{-5} \sim 10^{-3}$ in Fig. 2. The norm e of the landscape gradient is defined as

$$e = \left\{ \frac{1}{L} \sum_m \sum_{l=1}^{L} \left[\frac{\delta J}{\delta u_m(l\Delta t)} \right]^2 \right\}^{1/2}. \qquad (22)$$

The proportion of optimization searches being practically trapped at various values of u_0 and e is determined by 100 runs and given in Fig. 2, with two different time resolutions of $L = 5$ and 10. Generally, the search is more likely to escape the trapping region when greater magnitude initial controls are chosen, and a more precise convergence threshold is employed. No fundamental difference is observed for the two time resolution values of $L = 5$ and 10 with the other parameters fixed, implying that the discretization constraints do not affect the landscape structure significantly even for $L = 5$. For this particular problem, the accumulation of larger numerical error in the case of $L = 5$ actually eases the deviation from the trapping region, according to the statistical data presented here. In Fig. 3 we selected 20 initial controls for each distinct u_0, optimized them until $J > 0.99$, and then recorded the mean field strengths $u_{\text{opt}} = \overline{|u_m|}$ of each component at the global optimum, which turned out to be much larger than the easily trapped initial field strengths in Fig. 2. Therefore, if the field strengths of the initial control are sufficiently large, i.e., comparable to those of global optimal control fields for the landscape, the trapping region will be very unlikely to halt the search. This

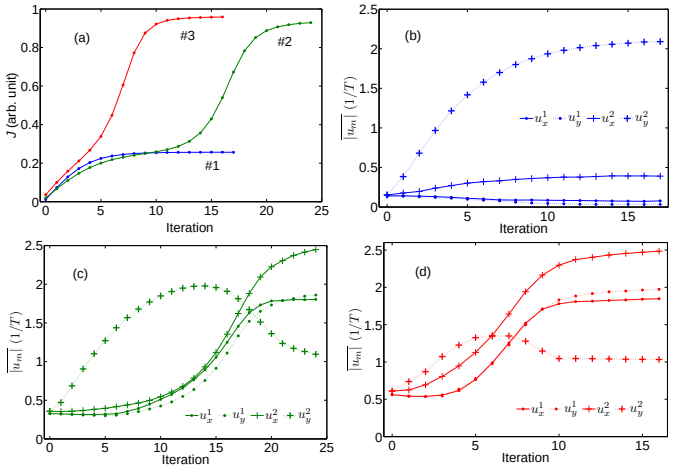

Fig. 1 (Color online) Three experimental gradient ascent trajectories on the control landscape of the two-spin sample of $^{13}CHCl_3$, starting from constant initial fields with different magnitudes. (a) The optimization of the objective value J. Trajectory #1 is terminated when J drops in the last iteration, while the other two approach the global maximum. (b)-(d), respectively for trajectories #1, #2 and #3, showing the evolution of the mean field strength $\overline{|u_m|}$ of each component, u_x^1,u_y^1,u_x^2 and u_y^2, in the optimization processes (given in the unit of T^{-1}).

phenomenon was also observed elsewhere[9,19] and is expected to widely apply, consistent with large numbers of reported successful simulations.[13,25]

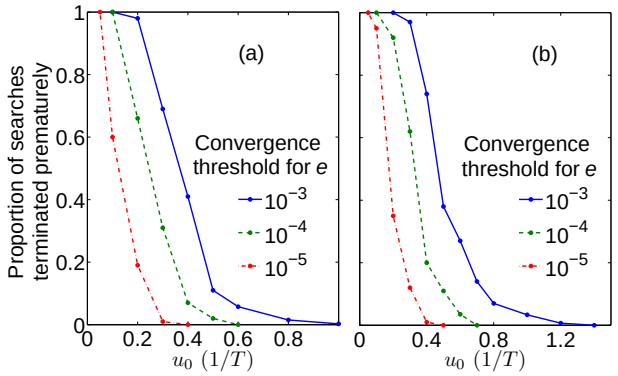

Fig. 2 (Color online) Simulation results from a model of the experimental two-spin system, showing the proportion of searches in 100 runs that are terminated prematurely at around $J = 0.25$ for various initial field strengths u_0 and convergence thresholds for the gradient norm e. (a) and (b) correspond to time resolution of $L = 5$ and 10, respectively.

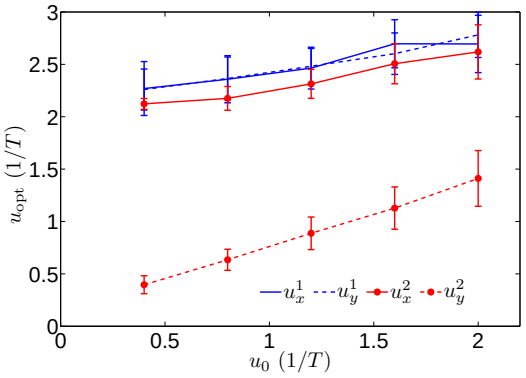

Fig. 3 (Color online) The mean field strengths of globally optimal controls ($J > 0.99$) of the two-spin landscape problem, obtained by optimizing from initial controls with different strengths u_0 in simulation.

Furthermore, we also numerically explored the higher-order landscape topology about the trap associated with trajectory #1 to check whether it is actually a local maximum. We randomly picked large numbers of perturbation directions $\delta u(\cdot)$ within the Hessian null space at a trap (including all four field components), and calculated the change of J when the control $u_{\rm trap}$ was varied along these directions. For sufficiently small variation, J is dominated by its lowest-order nonzero derivative along δu. It is found that in a small neighborhood around $u_{\rm trap}$ we have $J(u_{\rm trap} + x\delta u) \approx J(u_{\rm trap}) + k_4 x^4$, where x is the distance from $u_{\rm trap}$ in the control space. The coefficient k_4 can be positive or negative depending on the direction δu, with two representative cases plotted in Fig. 4. The numerical evidence implies that within the Hessian null space at the trap, the third derivative of J is zero while the fourth is indefinite. Thus, the trap identified in the two-spin example is actually only a trap to second order, but not a true local maximum.

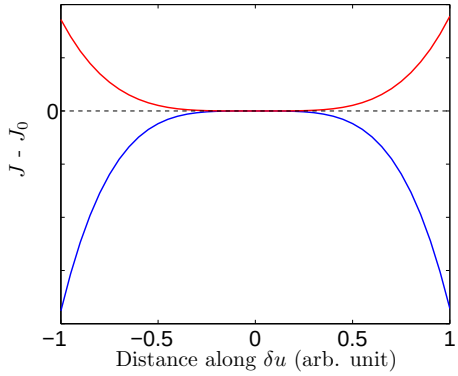

Fig. 4 (Color online) The second-order trap in the two-spin problem is shown *not* to be a local maximum. As we perturb a trap control $u_{\rm trap}$ along different directions δu in the Hessian null space, J may either increase or decrease from the value J_0 of the trap as a quartic function of the distance from $u_{\rm trap}$, as the representative red and blue curves respectively show.

5 Discussion and Conclusions

This paper mainly considers the control landscape for Ising linear spin chain systems, and derives the sufficient condition for a type of suboptimal traps of at least second order over the landscape caused by singularity. The results extend the understanding of the role of singular controls in landscape analysis. For quantum systems controlled by multiple fields, turning off some field components can produce singular controls of various degrees. The problem analyzed in this paper provides an example in which the singular traps exist as a continuously varying manifold over the nonzero field components involved, and the distinct members of which can be identified by performing simple gradient optimization from some particularly chosen initial controls. To illustrate the theoretical conclusions, we performed NMR experiments with a heteronuclear two-spin molecule, and observed the influence of the predicted singular trap on practical gradient searches. Additional numerical simulations showed how the choice of initial controls influences the likelihood of being trapped in practice, and that the trap is actually not a local optimum when higher-order derivatives are taken into consideration. For the three-spin case we compared two different physical models of linear and triangular internuclear couplings, suggesting that the singular traps may disappear when more complex couplings are present in a set of spins. In optimal control experiments with spin systems the presence of landscape singularity could be a factor of significance. However, the influence of zero field traps appear easy to be avoided by starting with simple physically motivated initial choices for controls, based on the expectation that each coupled spin may have some role in the optimal dynamics.

The advances in this work are best understood in the overall context of control landscape principles. As stated in the Introduction, these principles rest on the satisfaction of three assumptions. The first assumption (i) on controllability and the second assumption (ii) on surjectivity concern inherent properties of the quantum system under control. The third assumption (iii) on complete access to all possible controls can never be fully satisfied, but the practical issue is having adequate control resources

to meet the dynamic objective; while significant violation of this practical criterion will eventually lead to traps,[14] reasonable considerations from spectroscopy appear to often provide guidance to identify suitable resources. Although the controllability assumption (i) is likely to be satisfied, violations can lead to traps on the landscape.[7] The surjectivity assumption (ii) is perhaps the least understood, and the present work along with prior studies[2,17,18] have identified singular control induced traps existing only as zero (or constant) fields, which are unusual experimentally where propagating fields naturally arise as controls. Simple physically based trial fields can easily avoid constant field traps, as shown here and in other works.[9] A recent study introduced a special algorithm to specifically seek singular controls, and none of the discovered singular controls (all were non-constant) corresponded to traps.[8] Additionally extensive careful simulations for state preparation,[13] optimization of general observables,[9] and the creation of targeted unitary transformations[25] also did not encounter any fields corresponding to traps on the landscape while on the way to reaching high fidelity control performance. Interestingly, all of the known cases with singular control induced traps are simple systems with sparse coupling (e.g., Ising spin systems in the present paper). The greater body of simulation studies,[13,25] which do not encounter traps of any type, generally have Hamiltonians with more complex coupling structure. The landscape findings in the present work upon going from a three-spin linear chain to the triangular coupling arrangement can also be viewed as increasing coupling complexity. These collective results suggest that trap-inducing singular controls are a rarity, especially in systems of extensive coupling complexity. Most importantly, further study is needed to fully understand the circumstances when any of the three landscape assumptions break down and produce control outcomes that encroach on the nominal favorable landscape topology.

References

1 C. Brif, R. Chakrabarti, and H. Rabitz, *New J. Phys.*, 2010, **12**, 075008.

2 A. N. Pechen and D. J. Tannor, *Phys. Rev. Lett.*, 2011, **106**, 120402.

3 H. Rabitz, T.-S. Ho, R. Long, R. Wu and C. Brif, *Phys. Rev. Lett.*, 2012, **108**, 198901.

4 A. N. Pechen and D. J. Tannor, *Phys. Rev. Lett.*, 2012, **108**, 198902.

5 V. Ramakrishna, M. V. Salapaka, M. Dahleh, H. Rabitz and A. Peirce, *Phys. Rev. A: At., Mol., Opt. Phys.*, 1995, **51**, 960–966.

6 S. G. Schirmer, H. Fu and A. I. Solomon, *Phys. Rev. A: At., Mol., Opt. Phys.*, 2001, **63**, 063410.

7 R.-B. Wu, M. A. Hsieh and H. Rabitz, *Phys. Rev. A: At., Mol., Opt. Phys.*, 2011, **83**, 062306.

8 R.-B. Wu, R. Long, J. Dominy, T.-S. Ho, and H. Rabitz, *Phys. Rev. A: At., Mol., Opt. Phys.*, 2012, **86**, 013405.

9 G. Riviello, C. Brif, R. Long, R.-B. Wu, K. M. Tibbetts, T.-S. Ho and H. Rabitz, *Phys. Rev. A: At., Mol., Opt. Phys.*, 2014, **90**, 013404.

10 H. A. Rabitz, M. M. Hsieh and C. M. Rosenthal, *Science*, 2004, **303**, 1998–2001.

11 T.-S. Ho and H. Rabitz, *J. Photochem. Photobiol. A: Chem.*, 2006, **180**, 226–240.

12 R. Wu, H. Rabitz and M. Hsieh, *J. Phys. A: Math. Theor.*, 2008, **41**, 015006.

13 K. W. Moore and H. Rabitz, *Phys. Rev. A: At., Mol., Opt. Phys.*, 2011, **84**, 012109.

14 K. M. Tibbetts and H. Rabitz, *Phys. Chem. Chem. Phys.*, 2015, **17**, 3164–3178.

15 A. Donovan, V. Beltrani and H. Rabitz, *Chem. Phys.*, 2013, **425**, 46–54.

16 A. Donovan, V. Beltrani and H. Rabitz, *J. Math. Chem.*, 2014, **52**, 407–429.

17 R. Chakrabarti and H. Rabitz, *Int. Rev. Phys. Chem.*, 2007, **26**, 671–735.

18 P. de Fouquieres and S. G. Schirmer, *Infin. Dimens. Anal. Quantum. Probab. Relat. Top.*, 2013, **16**, 1350021.

19 A. N. Pechen and D. J. Tannor, *Isr. J. Chem.*, 2012, **52**, 467–472.

20 M. Nimbarkar, R. Zeier, J. L. Neves, S. B. Elavarasi, H. Yuan, N. Khaneja, K. Dorai and S. J. Glaser, *Phys. Rev. A: At., Mol., Opt. Phys.*, 2012, **85**, 012325.

21 S. Bose, *Phys. Rev. Lett.*, 2003, **91**, 207901.

22 G. A. Morris and R. Freeman, *J. Am. Chem. Soc.*, 1979, **101**, 760–762.

23 Q. Sun, I. Pelczer, G. Riviello, R.-B. Wu and H. Rabitz, *Phys. Rev. A: At., Mol., Opt. Phys.*, 2014, **89**, 033413.

24 Q. Sun, I. Pelczer, G. Riviello, R.-B. Wu and H. Rabitz, *Phys. Rev. A: At., Mol., Opt. Phys.*, 2015, **91**, 043412.

25 K. W. Moore, R. Chakrabarti, G. Riviello and H. Rabitz, *Phys. Rev. A: At., Mol., Opt. Phys.*, 2011, **83**, 012326.

26 R. Wu, A. Pechen, H. Rabitz, M. Hsieh and B. Tsou, *J. Math. Phys.*, 2008, **49**, 022108.

27 L. M. K. Vandersypen and I. L. Chuang, *Rev. Mod. Phys.*, 2005, **76**, 1037–1069.

28 O. W. Sorensen, G. W. Eich, M. H. Levitt, G. Bodenhausen and R. R. Ernst, *Prog. Nucl. Magn. Reson. Spectrosc.*, 1983, **16**, 163–192.

29 K. W. M. Tibbetts, C. Brif, M. D. Grace, A. Donovan, D. L. Hocker, T.-S. Ho, R.-B. Wu and H. Rabitz, *Phys. Rev. A: At., Mol., Opt. Phys.*, 2012, **86**, 062309.

30 Z. Li, H. Zhou, C. Ju, H. Chen, W. Zheng, D. Lu, X. Rong, C. Duan, X. Peng and J. Du, *Phys. Rev. Lett.*, 2014, **112**, 220501.

31 N. Khaneja, T. Reiss, C. Kehlet, T. Schulte-Herbrüggen and S. J. Glaser, *J. Magn. Reson.*, 2005, **172**, 296–305.

32 I. Wong, A. Grigoriu, J. Roslund, T.-S. Ho and H. Rabitz, *Phys. Rev. A: At., Mol., Opt. Phys.*, 2011, **84**, 053429.

33 N. Khaneja, R. Brockett and S. J. Glaser, *Phys. Rev. A: At., Mol., Opt. Phys.*, 2001, **63**, 032308.